Table 1. Correlations between fit parameters (data at 400 nm) for reflection ellipsometry data only and for both reflection and transmission ellipsometry data combined. The correlation between parameters when both data sets are used is significantly reduced compared to that when only reflection ellipsometry data are used.

	Reflection only			
	n_e	k_e	n_o	k_o
n_e	1.000	–0.79	0.981	0.989
k_e	–0.79	1.000	–0.890	–0.689
n_o	0.981	–0.890	1.000	0.943
k_o	0.989	–0.689	0.943	1.000
	Reflection and transmission			
	n_e	k_e	n_o	k_o
n_e	1.000	0.139	0.835	0.575
k_e	0.139	1.000	–0.100	0.690
n_o	0.835	–0.100	1.000	0.384
k_o	0.575	0.690	0.384	1.000

electroluminescent conjugated polymers. As an example, Figure 3 shows the anisotropic optical constants of a film of F8BT. The ordinary absorption was again in good agreement with the spectrum obtained from normal incidence transmission measurements. Although not as anisotropic as OC1C10–PPV, F8BT shows considerable anisotropy, with a birefringence of 0.19 at 633 nm. As with OC1C10–PPV there is a slight blue shift in the absorption peaks for the extraordinary direction with respect to the ordinary direction, again indicating a decreased conjugation length for chains lying out of the plane of the film.

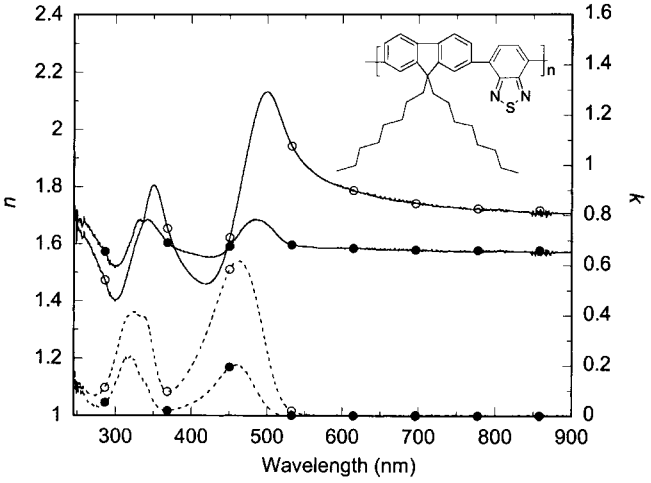

Fig. 3. The ordinary (○) and extraordinary (●) values for n (solid lines) and k (dotted lines) for F8BT. The chemical structure of F8BT is inset.

In conclusion, we have shown that a combination of reflection and transmission ellipsometry can be reliably employed to determine the ordinary and extraordinary optical constants in conjugated polymer films in both the absorbing and transparent regions. We have presented optical constants for two commonly used electroluminescent polymers, which will be useful in optical modeling of LEDs and photovoltaic devices. The technique provides structural information about the degree of chain alignment, and will in the future be applied to study the effects of annealing on optical properties, and to investigate possible variation of anisotropy with film thickness in thinner films than were studied here.

Experimental

OC1C10–PPV and F8BT were spin-coated on 1.2 mm Spectrosil-B substrates. Spectrosil-B has well-known optical constants, with negligible refractive index dispersion and no absorption over the wavelength range of interest. The OC1C10–PPV film was spin-coated from a chloroform solution at a concentration of 5 g/L and the F8BT film from a xylene solution at 15 g/L. The samples were annealed for 14 h at 115 °C in vacuum.

Measurements were performed using a J. A. Woollam M-2000 diode-array rotating-compensator ellipsometer, with a xenon lamp source. The rotating compensator system does not suffer from regions that are insensitive to Δ, unlike rotating-polarizer or rotating-analyzer systems, which are insensitive around $\Delta = 0°$ and $\Delta = 180°$. This meant that Δ_t, which was always close to 0° in this experiment, was not affected by excessive noise. Reflection and transmission ellipsometry measurements were performed in air over a wavelength range of 245 nm–900 nm. The angles of incidence used were between 55° and 70° for reflection ellipsometry and between 40° and 60° for transmission ellipsometry, in steps of 5°. No evidence for biaxial anisotropy within the plane of the film was observed either by rotating the sample in the plane of the film, or from non-zero off-diagonal elements in the Jones matrix describing the sample response.

Received: June 8, 2001
Final version: October 17, 2001

[1] W. M. V. Wan, N. Greenham, R. H. Friend, *J. Appl. Phys.* **2000**, *87*, 2542.
[2] D. McBranch, I. H. Campbell, D. L. Smith, J. P. Ferraris, *Appl. Phys. Lett.* **1995**, *66*, 1175.
[3] R. Burzynski, P. N. Prasad, F. E. Karasz, *Polymer* **1990**, *31*, 627.
[4] R. W. Gymer, R. H. Friend, H. Ahmed, P. L. Burn, A. M. Kraft, A. B. Holmes, *Synth. Met.* **1993**, *57*, 3683.
[5] T. Kawase, D. J. Pinner, R. H. Friend, T. Shimoda, *Synth. Met.* **2000**, *111–112*, 583.
[6] E. K. Miller, M. D. McGehee, M. Diaz-Garcia, V. Srikant, A. J. Heeger, *Synth. Met.* **1999**, *102*, 1091.
[7] J. Sturm, S. Tasch, A. Niko, G. Leising, E. Toussaere, J. Zyss, T. C. Kowalczyk, K. D. Singer, U. Scherf, J. Huber, *Thin Solid Films* **1997**, *298*, 138.
[8] R. Synowicki, *Thin Solid Films* **1998**, *313–314*, 394.
[9] L. A. A. Pettersson, T. Johansson, F. Carlsson, H. Arwin, O. Inganäs, *Synth. Met.* **1999**, *101*, 198.
[10] D. Comoretto, G. Dellepiane, F. Marabelli, J. Cornil, D. A. dos Santos, J. L. Brédas, D. Moses, *Phys. Rev. B* **2000**, *62*, 10 173.
[11] E. K. Miller, D. Yoshida, C. Y. Yang, A. J. Heeger, *Phys. Rev. B* **1999**, *59*, 4661.

Low-Temperature Growth of Well-Aligned ZnO Nanorods by Chemical Vapor Deposition**

By *Jih-Jen Wu** and *Sai-Chang Liu*

One-dimensional nanometer-sized semiconductor materials, i.e., nanowires and nanorods, have attracted considerable attention due to their great potential for fundamental studies of the roles of dimensionality and size in their physical proper-

[*] Prof. J.-J. Wu, S.-C. Liu
Department of Chemical Engineering
National Cheng Kung University
Tainan (Taiwan)
E-mail: wujj@mail.ncku.edu.tw

[**] This work was supported by the National Science Council, Taiwan, under contract no. NSC-90-2214-E006-023.

  0935-9648/02/0302-0215 $ 17.50+.50/0

ADVANCED MATERIALS

ties as well as for their application in optoelectronic nanodevices.[1] The growth of group IV, III–V, and II–VI semiconductor nanowires has been demonstrated by various methods, including the vapor–liquid–solid (VLS) growth mechanism,[2] oxide-assisted growth,[3] and template-based growth methods.[4] In addition, the growth of SiCN nanorods[5] and GaN nanowires[6] via the native nanocrystal-seeded method has also been reported. ZnO exhibits a direct bandgap of 3.37 eV at room temperature with a large exciton binding energy of 60 meV. The strong exciton binding energy, which is much larger than that of GaN (25 meV) and the thermal energy at room temperature (26 meV), can ensure an efficient exciton emission at room temperature under low excitation energy.[7] As a consequence, ZnO is recognized as a promising photonic material in the blue-UV region. Room-temperature UV lasing properties have recently been demonstrated from ZnO epitaxial films, microcrystalline thin films, and nanoclusters.[8] The synthesis of one-dimensional single-crystalline ZnO nanostructures has been of growing interest owing to their promising application in nanoscale optoelectronic devices. Single-crystalline ZnO nanowires have been synthesized successfully using high-temperature VLS growth methods.[9] Room-temperature UV lasing in ZnO nanowires has been demonstrated very recently.[10] Single-crystalline ZnO nanobelts have been prepared by simply evaporating the ZnO powders at a high temperature of 1400 °C.[11] However, for practical applications, high-density and well-ordered nanostructures will be needed. Here, we present a simple chemical vapor deposition (CVD) approach to the growth of well-aligned ZnO nanorods at a low temperature of around 500 °C. Structural characterization of the ZnO nanorods by X-ray diffraction (XRD) and transmission electron microscopy (TEM) indicates that the nanorods are preferentially oriented in the *c*-axis direction. Photoluminescence (PL) characteristics of the ZnO nanorods show a strong UV light emission peaking at around 386 nm at room temperature.

ZnO nanorods were grown in a two-temperature-zone furnace. Zinc acetylacetonate hydrate ($Zn(C_5H_7O_2)_2{\cdot}x\,H_2O$), which has been used to grow ZnO whiskers and films,[12] was vaporized at 130–140 °C in a furnace. The vapor was carried by a N_2/O_2 flow into the higher temperature zone of the furnace in which substrates were located. ZnO nanorods were grown directly on bare fused silica or silicon substrates at a temperature of 500 °C. As shown in Figure 1, a high density of well-aligned nanorods with a diameter in the range 60–80 nm formed uniformly over the entire substrate at a vaporizing temperature of 135 °C. The energy dispersive spectrometry (EDS) of the nanorods shows that the atomic composition ratio of Zn/O is about 1:1. Size control of the well-aligned ZnO nanorod diameters was achieved by adjusting the vaporizing temperatures of zinc acetylacetonate hydrate.

The crystal structure of the nanorods was examined by XRD. Figure 2 shows a typical XRD pattern of the well-aligned ZnO nanorods grown on a fused silica substrate. The two peaks are indexed as (0002) and (0004) of the wurtzite structure of ZnO, indicating that the nanorods are preferen-

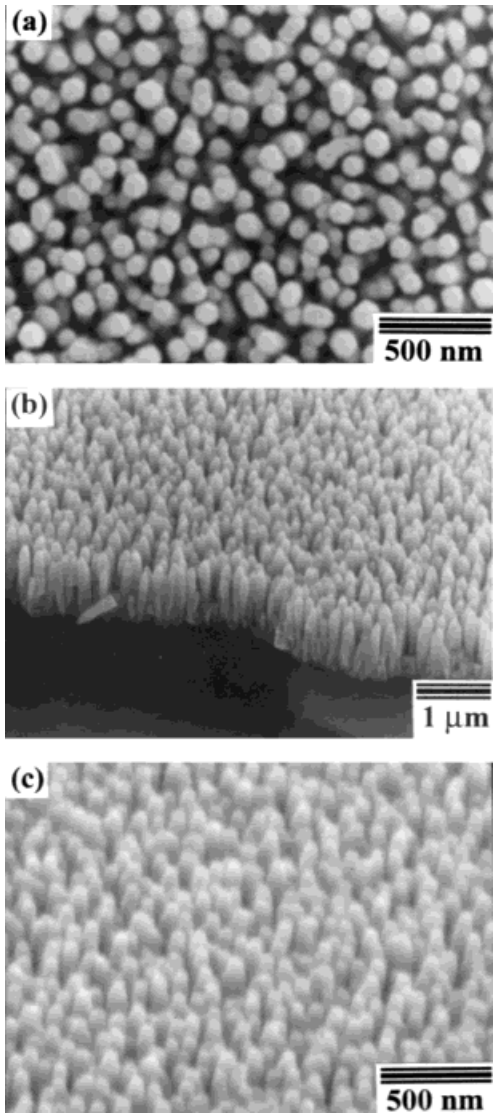

Fig. 1. SEM images of ZnO nanorods grown on fused silica substrates at a vaporizing temperature of 135 °C. a) Top view, b,c) 45° tilted view.

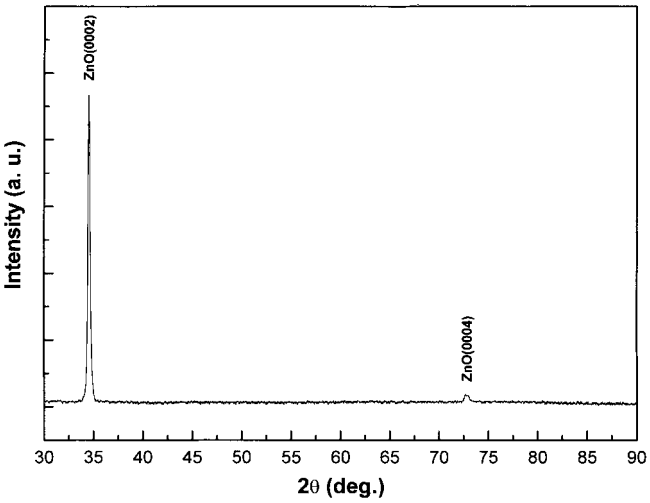

Fig. 2. XRD pattern of ZnO nanorods on a fused silica substrate.

  0935-9648/02/0302-0216 $ 17.50+.50/0

tially oriented in the *c*-axis direction. In contrast to the XRD spectra of the ZnO nanowires grown using the VLS mechanism[9] wherein the diffraction peaks of the catalyst or the zinc metal appeared with the ZnO peaks, pure ZnO phase is synthesized on the substrates in our case.

Further structural characterization of the ZnO nanorods was performed using TEM. Figure 3a shows a cross-sectional image of the ZnO nanorods, which were grown on a fused silica substrate, with a diameter in the range 80–100 nm. It reveals that all nanorods grew in a direction perpendicular to the substrate. Moreover, no additional metal particle appeared on the top or the bottom of the rods, implying a non-VLS approach to the growth of the well-aligned ZnO nanorods at a low temperature was achieved. Typical bright-field and dark-field images of the ZnO nanorods are illustrated in Figure 3b and Figure 3c, respectively. The dark-field image indicates that the nanorod possesses the single crystalline structure. Figure 3d shows a high-resolution TEM image of a nanorod. The lattice spacing of 0.257 nm corresponds to the *d*-spacing of (0002) crystal planes, confirming the XRD analysis that the ZnO nanorods are preferentially oriented in the *c*-axis direction, as shown in Figure 2.

PL spectra of the ZnO nanorods were measured on a fluorescence spectrophotometer using a Xe lamp with an excitation wavelength of 325 nm at room temperature. Figure 4 shows the PL spectrum of the ZnO nanorods with a diameter in the range 60–80 nm. Three emitting bands, including a strong ultraviolet emission at around 386 nm, a very week blue band (440–480 nm), as well as an almost negligible green band (510–580 nm), were observed. The UV emission must be contributing to the near band edge emission of the wide band-gap ZnO. It has been suggested that the green band emission corresponds to the singly ionized oxygen vacancy in ZnO and results from the recombination of a photogenerated hole with the single ionized charge state of this defect.[13] The stronger the intensity of the green luminescence, the more singly ionized oxygen vacancies there are. Thus the almost negligible green band in Figure 4 shows that there is a very low concentration of oxygen vacancies in the well-aligned ZnO nanorods. The observation of blue band emission (440–480 nm) of ZnO film has been also reported using cathodoluminescence.[14] However, the mechanism of this emission is not yet clear.

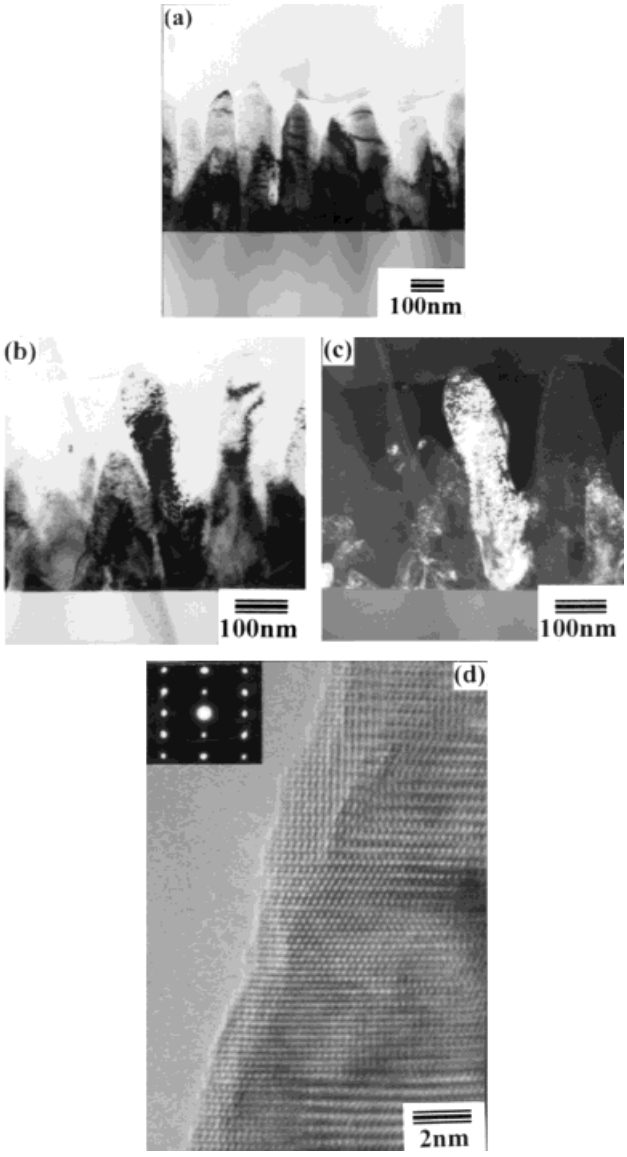

Fig. 3. TEM cross-sectional images of ZnO nanorods grown on fused silica substrates at a vaporizing temperature of 138 °C. a) Low-magnification image shows nanorods grown with a direction perpendicular to the substrate. b,c) Typical bright-field and dark-field images of the ZnO nanorods, respectively. d) High-resolution TEM image of a single-crystalline ZnO nanorod and the corresponding electron diffraction pattern (inset).

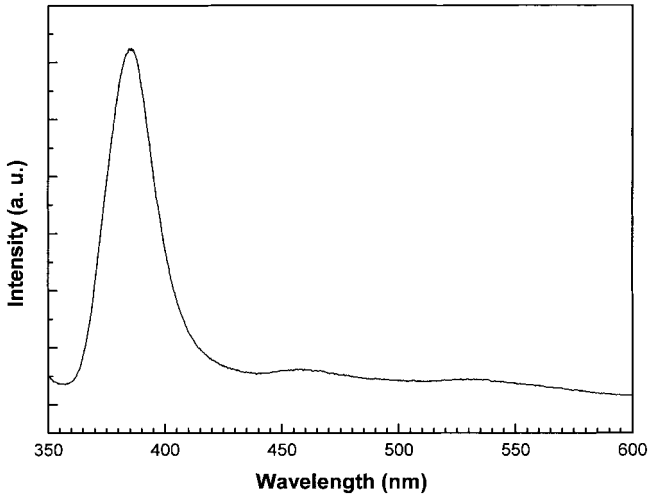

Fig. 4. Typical photoluminescence spectrum of ZnO nanorods.

A simple CVD method for the growth of the well-aligned ZnO nanorods at low temperature has been demonstrated in this report. The nanorods grown on fused silica are preferentially oriented in the *c*-axis direction. PL characteristics of the ZnO nanorods show a strong UV light emission peaking at around 386 nm at room temperature. We believe the presented approach is a simple one for practical application to nanoscale optoelectronic devices.

  0935-9648/02/0302-0217 $ 17.50+.50/0

ADVANCED MATERIALS

Experimental

ZnO nanorods were grown in a two-temperature-zone furnace. Silicon wafers and fused silica plates were employed as solid reactant susceptors or substrates. They were cleaned in an ultrasonic bath of acetone for 20 min. Zinc acetylacetonate hydrate ($Zn(C_5H_7O_2)_2{\cdot}x\,H_2O$, Lancaster, 98 %) placed on a cleaned silicon susceptor was loaded into the low temperature zone of the furnace, which was controlled to be in the range 130–140 °C to vaporize the solid reactant. The vapor was carried by a 500 sccm N_2/O_2 flow into the higher temperature zone of the furnace in which substrates were located at 200 torr. ZnO nanorods were grown directly on bare fused silica or silicon substrates at a temperature of 500 °C.

The morphology and size distribution as well as elemental analyses of the nanorods were examined using a scanning electron microscope (SEM) (Hitachi, S-4200) equipped with an EDS. The crystal structure of the nanorods was analyzed using XRD (Rigaku) and HRTEM (JEOL, JEM-4000EX). PL studies were conducted using a Hitachi F-4500 fluorescence spectrophotometer with a Xe lamp at room temperature. The excitation wavelength was 325 nm.

Received: July 23, 2001
Revised: September 10, 2001

[1] C. M. Lieber, *Solid State Commun.* **1998**, *107*, 607.
[2] a) J. Westwater, D. P. Gosain, S. T.omiya, S. Usui, H. Ruda, *J. Vac. Sci. Technol. B* **1997**, *15*, 554. b) A. M. Morales, C. M. Lieber, *Science* **1998**, *279*, 208.
[3] a) N. Wang, Y. F. Zhang, Y. H. Tang, C. S. Lee, S. T. Lee, *Appl. Phys. Lett.* **1998**, *73*, 3902. b) W. S. Shi, Y. F. Zheng, N. Wang, C. S. Lee, S. T. Lee, *Appl. Phys. Lett.* **2001**, *78*, 3304.
[4] a) W. Han, S. Fan, Q. Li, Y. Hu, *Science* **1997**, *277*, 1287. b) J. Zhu, S. Fan, *J. Mater. Res.* **1999**, *14*, 1175.
[5] F. G. Tarntair, C. Y. Wen, L. C. Chen, J. J. Wu, K. H. Chen, P. F. Kuo, S. W. Chang, Y. F. Chen, W. K. Hong, H. C. Cheng, *Appl. Phys. Lett.* **2000**, *76*, 2630.
[6] M. He, I. Minus, P. Zhou, S. N. Mohammed, J. B. Halpern, R. Jacobs, W. L. Sarney, L. Salamanca-Riba, R. D. Vispute, *Appl. Phys. Lett.* **2000**, *77*, 3731.
[7] a) Y. Chen, D. M. Bagnall, H. Koh, K. Park, K. Hiraga, Z. Zhu, T. Yao, *J. Appl. Phys.* **1998**, *84*, 3912. b) A. Ohtomo, M. Kawasaki, Y. Sakurai, I. Ohkubo, R. Shiroki, Y. Yoshida, T. Yasuda, Y. Segawa, H. Koinuma, *Mater. Sci. Eng. B* **1998**, *56*, 263.
[8] a) D. M. Bagnall, Y. F. Chen, Z. Zhu, T. Yao, S. Koyama, M. Y. Shen, T. Goto, *Appl. Phys. Lett.* **1997**, *70*, 2230. b) P. Zu, Z. K. Tang, G. K. L. Wong, M. Kawasaki, A. Ohtomo, H. Koinuma, Y. Segawa, *Solid State Commun.* **1997**, *103*, 459. c) H. Co, J. Y. Xu, E. W. Seelig, R. P. H. Chang, *Appl. Phys. Lett.* **2000**, *76*, 2997.
[9] a) M. H. Huang, Y. Wu, H. Feick, N. Tran, E. Weber, P. Yang, *Adv. Mater.* **2001**, *13*, 113. b) Y. C. Kong, D. P. Yu, B. Zhang, W. Fang, S. Q. Feng, *Appl. Phys. Lett.* **2001**, *78*, 407.
[10] M. H. Huang, S. Mao, H. Feick, H. Yan, Y. Wu, H. Kind, E. Weber, R. Russo, P. Yang, *Science* **2001**, *292*, 1897.
[11] Z. W. Pan, Z. R. Dai, Z. L. Wang, *Science* **2001**, *291*, 1947.
[12] a) M. Satoh, N. Tanaka, Y. Ueda, S. Ohshio, H. Saitoh, *Jpn. J. Appl. Phys.* **1999**, *38*, L586. b) K. Haga, F. Katahira, H. Watanabe, *Thin Solid Films* **1999**, *343–344*, 145.
[13] K. Vanheusden, W. L. Warren, C. H. Seager, D. R. Tallant, J. A. Voigt, B. E. Gnade, *J. Appl. Phys.* **1996**, *79*, 7983.
[14] Z. Fu, B. Lin, G. Liao, Z. Wu, *J. Cryst. Growth* **1998**, *193*, 316.

Metal Silicide/Silicon Nanowires from Metal Vapor Vacuum Arc Implantation**

By *Chi-Pui Li*, *Ning Wang*, *Sai-Peng Wong*, *Chun-Sing Lee*, and *Shuit-Tong Lee**

Silicon nanowires (SiNWs) are attracting much interest because they are expected to play an important role as interconnects and basic components for future mesoscopic electronic and optoelectronic devices.[1] Towards this end, controlling the electrical conductivity of SiNWs and patterning the electrical contact to SiNWs are major issues. Metal silicide (MS) is among the best candidates for the electrical contact to silicon.[2] Epitaxial MS with a good lattice matching with the Si substrate can result in greater stability.[3–5] The $NiSi_2$/Si and $CoSi_2$/Si systems have superior structural perfection[6] because of their small lattice mismatches (–0.4 % for $NiSi_2$/Si and –1.2 % for $CoSi_2$/Si). Ion beam synthesis (IBS) of MS by metal implantation into Si substrates has been used since the mid-1980s[7,8] because of its precise control of implantation dose and excellent reproducibility. However, the high dose requirement of the conventional IBS technique is a major drawback. To overcome this problem, metal vapor vacuum arc (MEVVA) ion source implantation[9] has been developed. In this paper, we report the synthesis of $NiSi_2$/Si and $CoSi_2$/Si on the surface of bare SiNWs using MEVVA implantation. This approach to the synthesis of metal silicide/Si nanowires (MS/SiNWs) can be potentially useful to fabricate electrical contacts to SiNWs and to improve the electrical conductivity of SiNWs.

SiNWs were synthesized by thermal decomposition of pure SiO powder (Aldrich, 325 mesh, 99.9 %)[10,11] at 1320 °C in an evacuated alumina tube for 7 h under a total pressure of 300 torr. The ambient gas consisted of Ar 95 % and H_2 5 % with a flow rate of 50 sccm. The dark brown and sponge-like SiNWs were obtained on the inside wall of the alumina tube. Without any treatment, SiNWs were then mounted on copper folding grids and directly implanted by MEVVA implantation with a nominal Ni^+ or Co^+ dose of 1×10^{17} cm^{-2} at an extraction voltage of 5 kV at room temperature. The MEVVA im-

[*] Prof. S. T. Lee, C. P. Li, Dr. C. S. Lee
Center of Super-Diamond and Advanced Films (COSDAF) &
Department of Physics and Materials Science
The City University of Hong Kong
Hong Kong SAR (China)
E-mail: apannale@cityu.edu.hk
Dr. N. Wang
Department of Physics
The Hong Kong University of Science and Technology
Hong Kong SAR (China)
Prof. S. P. Wong
Department of Electronic Engineering
The Chinese University of Hong Kong
Hong Kong SAR (China)

[**] The authors thank W. S. Shi and K. Ne. This work is supported in part by the Research Grants Council of Hong Kong (No. 9040459/HKUST1043/00P and 9040637/CityU1063/01P).

  0935-9648/02/0302-0218 $ 17.50+.50/0